NASA CONTRACTOR REPORT 166603

Laser Velocimeter Measurements of Dynamic Stall

F. K. Owen

CONTRACT NAS2- 11080

April 1984

NASA

NASA CONTRACTOR REPORT 166603

Laser Velocimeter Measurements of Dynamic Stall

F. K. Owen
Complere Inc.
P.O. Box 1697
Palo Alto, CA 94302

Prepared for
Ames Research Center
under Contract NAS2-11080

National Aeronautics and
Space Administration

Ames Research Center
Moffett Field California 94035

ABSTRACT

Laser velocimeter measurements of the unsteady flow over a NACA 0012 airfoil undergoing conditions of dynamic stall are reported. This work was undertaken in support of a program to determine unsteady pressure distributions and loads on an airfoil oscillating in a steady oncoming flow. Flowfield measurements around the static stall angle are evaluated and comparisons are made with laser holographic interferometry measurements. A complete tabulation of the laser velocimeter data are provided under separate cover.

INTRODUCTION

Almost all conceivable lifting situations occur on the blades of a helicopter rotor in flight. Conditions of attached flow and high-lift efficiency, shock-induced separation (advancing blade tip) and leading-edge separation (retreating blade) are encountered during each revolution. In certain flight conditions, large unsteady air loads on the blades of a helicopter are caused by the interaction between the rotating blades and intense vortices trailed from the tips of the preceding blades. Such unsteady blade loads determine the higher frequency stresses, the blade fatigue life, and the higher frequency noise of the helicopter rotor. These situations are further complicated by cyclic pitch and the time dependency and three dimensionality of the flow. To address these complicated flows, an improved understanding is needed of two-dimensional, time-dependent flow cases. At present, we cannot predict flows caused by shock-induced or leading edge separation. This is due largely to inaccurat turbulence models for the turbulent separated viscous layer and the near-wake. Measurements of the mean and transport properties of these highly turbulent separated flows are needed to develop improved turbulence models and hence better prediction methods. In the past, these measurements were difficult to make, but with recent development of combined nonintrusiv model surface, laser velocimeter and holographic measurements techniques, new information can now be obtained for these flows.

As a first step, then, experimental information is required for two-dimensional flows which produce conditions similar to those likely to be encountered in flight. An airfoil whose angle of attack is varied periodically in a steady oncoming flow is a good first approximation.

The purpose of this report is to describe the results obtained from measurements of the time-dependent flow fields which were generated in the NASA 2-ft wind tunnel by oscillating a NACA 0012 airfoil through an angle-of-attack range (-5 to +15°) in a M = 0.4 freestream flow. These results are also compared with holographic measurements (Ref. 1) to determine the feasibility of interferometer techniques for applications to nominally two-dimensional unsteady separated flow fields.

TIME DEPENDENT FLOW-FIELD MEASUREMENTS

Considerable attention and effort has already been directed to the area of conditional sampling as a means of revealing flow features which appear intermittently rather than continuously yet still have an important influence on flow structure and development. However, until recently, these efforts were all restricted to experiments in which the flow-field sensor had a continuous output which itself could be used to generate the criteria for the conditional averages; so that measurements were of necessity restricted to unidirectional shear flows in which, for example, standard hot-wire anemometry techniques could be used. Whole classes of flows, namely recirculating and unsteady wake flows have therefore been neglected. In these flows, it is extremely difficult to generate reliable analog or digital outputs with conventional flow-field instrumentation, since these flows are extremely sensitive to probe interference.

Unfortunately, laser velocimeter data alone are usually difficult to conditionally sample since in most cases the data rates are insufficient to generate real-time information from which the sampling criteria can be determined. A technique close to conditional sampling can be used to generate ensemble averages at given phase angles in turbulent flows

superimposed on periodic motions, such as those in reciprocating machinery or helicopter wakes, for example. In these cases, the sampling condition can be derived from a periodic timing signal. However, in the case of aerodynamic oscillations, whose period is not exactly constant, for example, the flows behind a bluff body, or oscillating airfoil, the sampling condition should be derived from the flow itself (Ref. 2). However, during this particular test an external pulse was used so that the data presented in this report will contain variations due to cycle-to-cycle flow repeatability, jitter. But we do not feel that the major conclusions will be affected.

EXPERIMENTAL DETAILS

Test Model

The experiment was conducted on a 2-D NACA 0012 model which consisted of a balsa wood core wrapped with 20 plies of graphite tape impregnated with epoxy resin. The airfoil which had a 15.24 cm chord and 61 cm span was mounted between the glass windows of the 2-ft wind tunnel test section by means of steel stubs which rode in needle bearings. There was a gap of approximately 1 mm between the wing and windows. The wing was pitched about the quarter chord by a Scotch yoke mechanism. The tests were conducted at freestream Mach numbers of between 0.3 and 0.6 at chord Reynolds numbers ranging from 0.5 to 2 million. Oscillatory tests were conducted at mean angles of attack of 5 and 10 degrees with amplitudes of $\pm$ 10 degrees at frequences up to 36 Hz. Laser velocimeter data were obtained at a freestream Mach number of 0.4 and chord Reynolds number of 1.5 million.

Laser Velocimeter

Velocity measurements were made with the laser velocimeter shown schematically in Fig. 1. This system was designed and built by NASA for the Ames 2x2-ft. transonic wind tunnel. This fringe-mode velocimeter is a dual-color system utilizing the 4880 and 5145 Angstrom lines of an argon-ion laser. One spectral line is used to measure the streamwise velocity component, the other to measure the vertical velocity component. Bragg-cell frequency shifting necessary for probing highly turbulent and separated flow regions is incorporated in both spectral lines. The frequency offsets also facilitate the direct measurement of the vertical velocity component (i.e., $\pm 45^\circ$ beam orientations to resolve the vertical velocity are unnecessary).

As seen in Fig. 1, most of the optical components are located outside the tunnel plenum chamber, where color separation, Bragg-cell frequency shifting, and the establishment of the four-beam matrix are accomplished. Only the transmitting optics, collecting lens, and photo detectors are mounted inside the plenum chamber. Two traversing systems are shown inside the plenum chamber. The one on the opposite side of the test section from the laser holds the collecting lens and photo detectors for forward-scatter light collection. The traversing system on the laser side of the test section supports the transmitting lenses. Mirrors fixed to this traversing system permit two-dimensional scanning of the velocimeter's sensing volume; the optics outside the plenum chamber remain stationary. Both traversing systems are driven with computer-controlled stepper motors. The effective sensing volume is approximately elliptic, 200 um in diamter and 3 mm long, with the axis aligned in the cross-stream direction.

Conditionally sampled, two-component laser-velocimeter measurements were obtained at reduced frequencies (wx/u) of .12 and 1.2. A schematic of the data reduction system is shown in Fig. 2 where signal processing is accomplished with single particle burst counters. In the system, a once-per-revolution pulse originated by the airfoil drive mechanism resets the multiplexer clock so that clock pulse number represents the instantaneous airfoil angle of attack throughout each cycle. Now, as particle arrival times are random the clock pulse number can be used to assign each velocity measurement to its correct phase ensemble. The two velocity components (u, v) and clock pulse number are recorded on floppy disc for analysis. Reynolds stress measurements were also obtained by requiring coincidence of the two velocity components before each data set was accepted. Software developed specifically for this test program enabled probability densities of each velocity component and velocity cross products to be determined for preselected angle-of-attck "windows." From this information, ensemble averages of the mean velocities $\overline{u}$, $\overline{v}$, and RMS values $\overline{u'}$ and $\overline{v'}$ and shear stress $\overline{u'v'}$ were calculated.

Naturally occurring particles in the tunnel are normally used for light scattering. In this facility, lubrication oil within the drive system vaporizes and then condenses in the tunnel circuit to provide a generous supply of scattering centers. Previous measurements across a normal shock have shown that these particles are small enough in size (estimated to be 1 μm) to give very good response to a step change in velocity at sonic speeds. At each point in the flow, generally several thousand velocity realizations are used to calculate the flow properties. However, to keep tunnel test time within reasonable limits, it was found necessary to seed the tunnel circuit in the present case, since we are

essentially measuring many different flow fields as the airfoil oscillates. Seeding was achieved using an artificial aerosol of Dioctylphalate of known size distribution which was generated with a Laskin nozzle generator and injected into the wind tunnel downstream of the test section. This aerosol had a count mean diameter of 0.7 μm (see Fig. 3).

RESULTS AND ANALYSIS

Phase averaged mean velocities and turbulence quantities were measured at two airfoil locations, namely, x/c = 0.45 and 1.06, i.e., at approximately mid-chord and in the near wake. Profiles were obtained at oscillation frequencies of 2.8 and 28 Hz, i.e., reduced frequencies of 0.12 and 1.2.

Ensemble-averaged axial velocity profiles are shown in Figs. 4-7. The most obvious feature of these results is the large hysteresis which exists as the airfoil oscillates in and out of stall. This hysteresis is even more pronounced at the higher frequency. In both cases, at x/c = .45, the flow is attached at ten degrees when the angle of attack is in increasing. Both flows are clearly stalled at 15 degrees with the 28 Hz case being more extensive. When the airfoil returns through 10 degrees, recovery appears more complete for the 2.8 Hz case.

In the near wake (x/c = 1.06) these differences are accentuated and the effect of frequency more pronounced. At ten degrees increasing angle of attack the low frequency profile shows a wider wake with a greater velocity deficit, an indication of earlier dynamic stall. At fifteen degrees, however, the higher frequency wake profile shows that much more extensive flow separation has occurred on the airfoil consistent with the x/c - .45 profiles. This indicates a significant loss of lift compared to the 2.8 Hz case. The profiles obtained as the airfoil retreats through

10 degrees clearly show the greater hysteresis in the 28 Hz case. Thus the essential flow-field features revealed by these profiles tell us that angle-of-attack oscillations through the static stall value produce significant flow-field hysteresis. Increasing the reduced frequency of oscillation delays the onset of dynamic stall but recovery is also delayed. This must result in a larger C_L hysteresis loop.

The measured axial velocity fluctuation levels presented in Figs. 4-7 are consistent with the mean profile observations. In the near wake at 10 degrees increasing angle of attack the RMS velocity fluctuations are significantly higher in the 2.8 Hz case, again an indication of earlier onset of dynamic stall. At 15 degrees the 28 Hz case shows higher turbulence levels even though the mean gradients in the wider wake are less. This indicates large-scale turbulent mixing and will be discussed later. Delayed stall recovery at 28 Hz is again evident at 10 degrees decreasing angle of attack since there is still evidence of much more extensive large-scale turbulence in the wake. Data taken on the airfoil confirm these trends. For completeness, phase-averaged mean and RMS vertical-velocity profiles are presented in Figs. 8-11. Although their interpretation is more difficult, on examination, similar trends are evident, namely, delayed stall onset and recovery for the case of higher reduced frequency. For the attached cases calculated flow angularity is consistent with airfoil angle of attack.

Although these ensemble mean and RMS velocity profiles give us a good deal of insight into this particular study of dynamic stall, further measurements are needed for us to assess turbulence models currently employed in dynamic stall prediction methods. The instantaneous velocity at a point in the flow may be expressed as

$$u = \bar{u} + u' + \tilde{u}$$

where $\bar{u}$ is the conventional mean, u' is the random fluctuation and $\tilde{u}$ is the unsteady contribution from the oscillating angle of attack. This term will vary in both amplitude and phase as a function of instantaneous angle of attack and reduced frequency. With a similar expression for the vertical velocity and insertion in the momentum equation we obtain

$$u\frac{\partial u}{\partial x} + v\frac{\partial u}{\partial y} = -\frac{1}{\rho}\frac{\partial p}{\partial x} + \nu\frac{\partial^2 u}{\partial y} - \frac{1}{\rho}\left(\overline{u'v'} + \overline{\tilde{u}\tilde{v}}\right)$$

if we asume that the random and time-dependent scales are uncorrelated.

The major assumption in all current unsteady calculations that the phase-averaged Reynolds stress distribution is related to the phase-averaged velocity profile as in the steady case

$$\langle u'v' \rangle = \epsilon\frac{\partial \langle u \rangle}{\partial y}, \quad \epsilon = \ell^2\left|\frac{\partial \langle u \rangle}{\partial y}\right|$$

We can see that this assumption is valid only if $\overline{u'v'}$ is unaffected by the oscillation and $\overline{u'v'} \gg \overline{\tilde{u}\tilde{v}}$.

A first attempt to determine the validity of these assumptions has been made by measuring tne ensemble-averaged Reynolds shear stresses in the near-wake region. The results for the case of 2.8 Hz are presented in Fig. 12. These averaged profiles show extremely high shear stress values in the dynamically stalled cases. Indeed, mixing length estimates obtained from these measured values and the slopes of the ensemble-averaged mean velocities indicate mixing lengths four to five times greater than those for steady stall cases (Ref. 3). This challenges the validity of the quasi-steady calculation procedures since it appears that the characteristic vortex shedding feature of dynamic stall leads to mixing

lengths significantly larger than those observed in the steady stall case. Unfortunately, since conventional averages were not taken, we cannot isolate the u v contribution directly.

This condition of vortex shedding also provides a stringent test case for laser holographic interferometry techniques as the basic assumption of zero normal pressure gradient used in deriving the Crocco relationship to determine velocity could be violated. This has been investigated in Ref. 1 where comparisons have been made between the laser velocimeter and holographic interferometer measurements. Velocity profiles at midchord and in the near wake are shown in Figs. 13-15, where it can be seen that, when the flow is attached, there is relatively good agreement between the two techniques even though the laser velocimeter data contain cycle to cycle "jitter." However, for the separated case, Fig. 14, agreement is poor, a consequence of strong normal pressure gradients in the flowfield.

CONCLUSIONS

An analysis of the measured ensemble averaged mean velocities, turbulent intensities and Reynolds shear stresses that occur during dynamic stall has been made. This analysis shows that significant flow field hysterisis is present around the static stall angle when the airfoil oscillates into and out of stall. This hysterisis is accentuated as the reduced frequency is increased.

The ensemble averaged mean profiles should provide challenging test cases for computation. However, the measured Reynolds shear stresses infer that characteristic vortex shedding, i.e., the sudden loss of circulation and lift, associated with dynamic stall produce mixing lengths

significantly larger than in the case of static stall. This fact challenges the basic quasi-steady assumptions currently employed in computational schemes. Consequently, the prediction of these flows will present a formidable challenge for many years to come.

Comparisons with the holographic interferometer results reveal an inherent weakness in the use of the Crocco relationship for the derivation of velocity profiles. This weakness is caused by the normal pressure gradients induced by the large-scale vortices associated with dynamic stall flowfields.

References

1. Lee, G., Buell, D. A., Licursi, J. and Craig, J. E. "Laser Holcgraphic Interferometry for Unsteady Airfoil Undergoing Dynamic Stall. AIAA paper no. 83-0388.

2. Owen, F. K. and Johnson, D. A. "Measurements of Unsteady Vortex Flowfields," AIAA Journal, Vol. 18, No. 10, 1980.

3. Johnson, D. A. "Transonic Flow Past a Symmetric Airfoil at High Angle of Attack," AAIA paper no. 79-1500R.

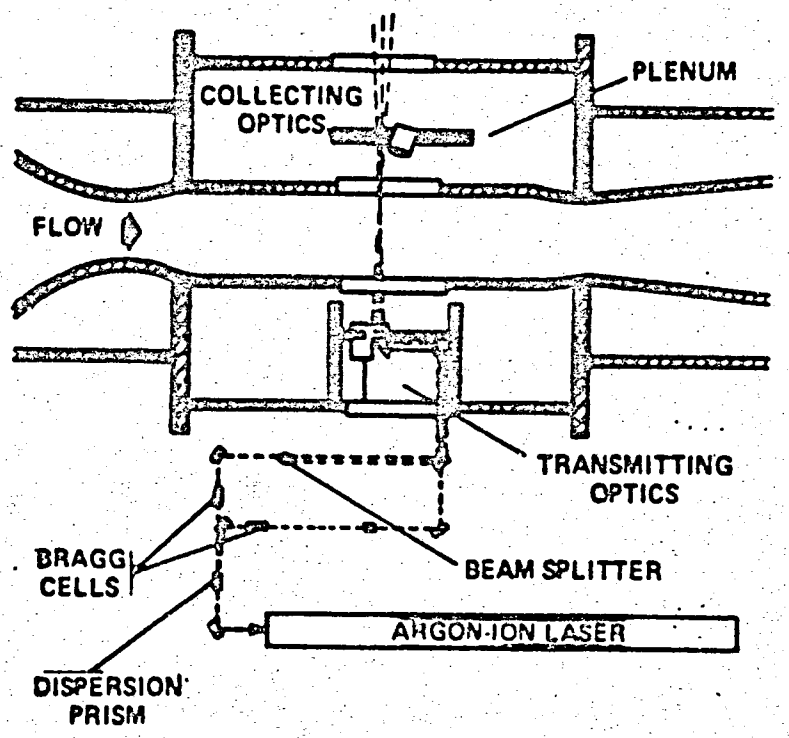

Fig. 1 Laser Velocimeter Installation in the Ames 2-foot Wind Tunnel.

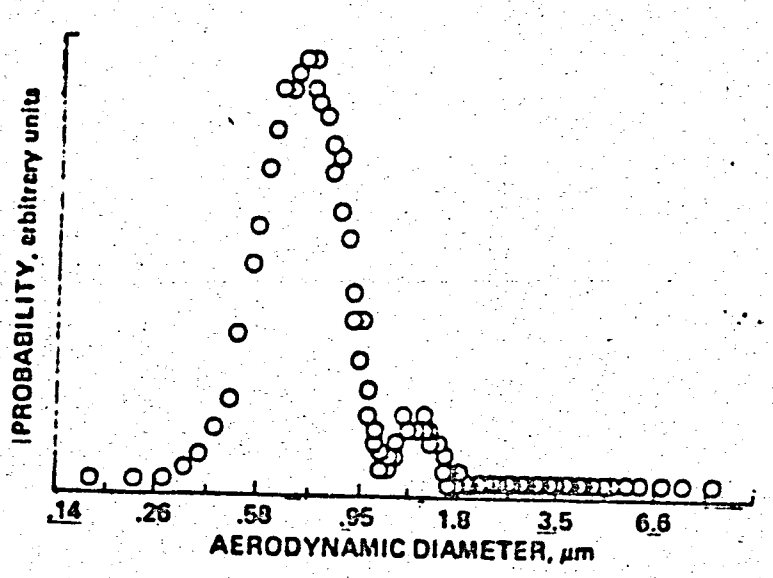

Fig. 3 Seed Particle Size Distribution.

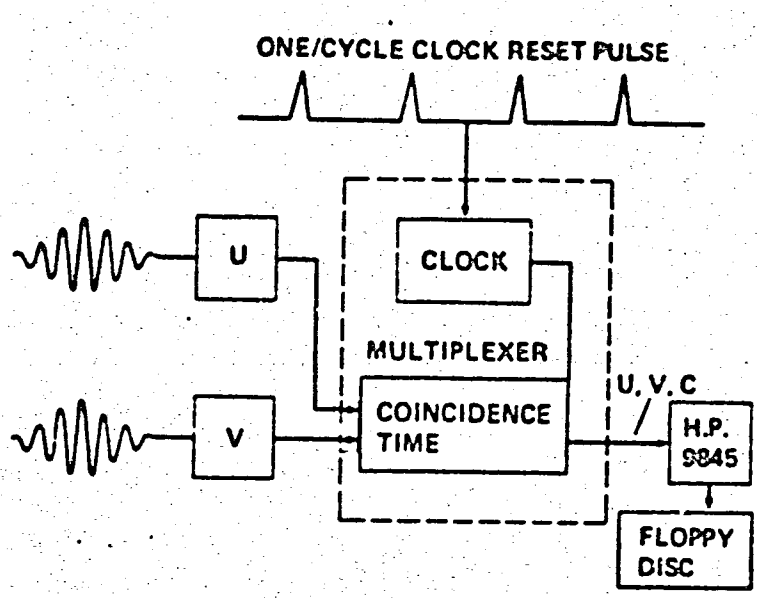

Fig. 2 Laser Velocimeter Processing Electronics for Studies of Dynamic Stall.

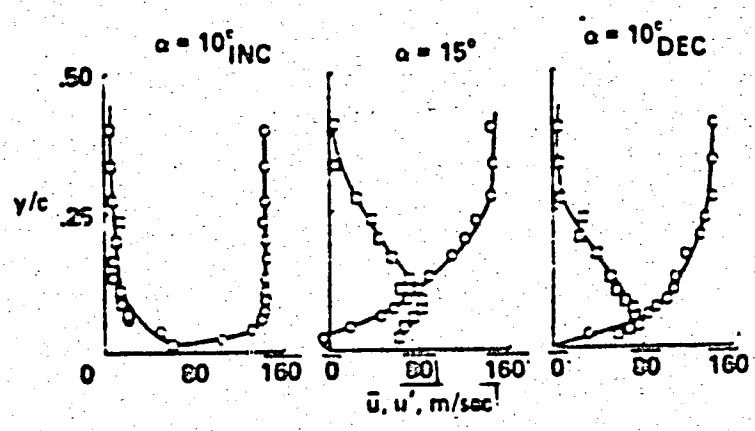

Fig. 4 Ensemble-Averaged Streamwise Mean and Turbulent Velocity Profiles at a Reduced Frequency of 0.12 (Circles Represent Mean Profiles) x/c = 0.45

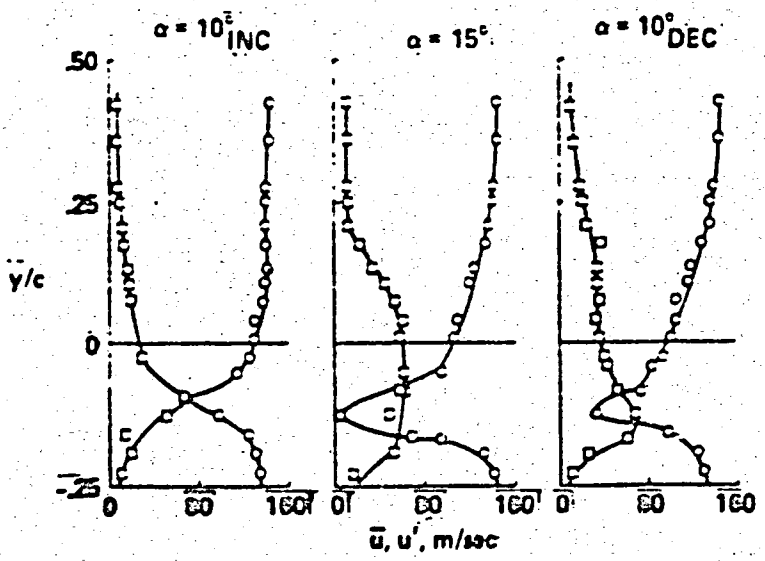

Fig. 5 Profiles for x/c = 1.06

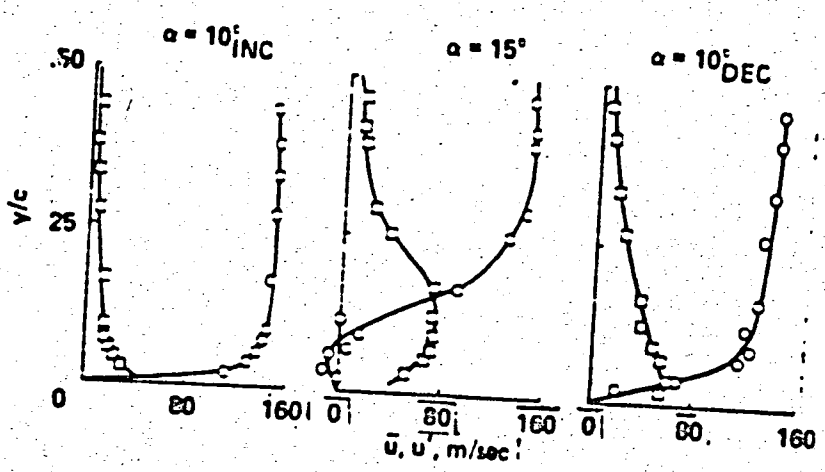

Fig. 6 Ensemble-Averaged Streamwise Mean and Turbulent Velocity Profiles at a Reduced Frequency of 1.2 (Circles Represent Mean Profiles) x/c = 0.45

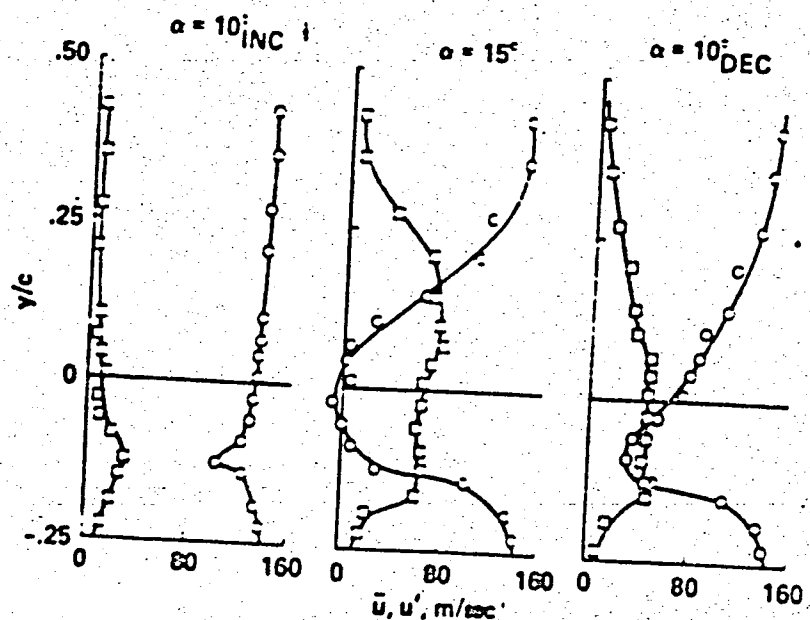

Fig. 7 Profiles for x/c = 1.06

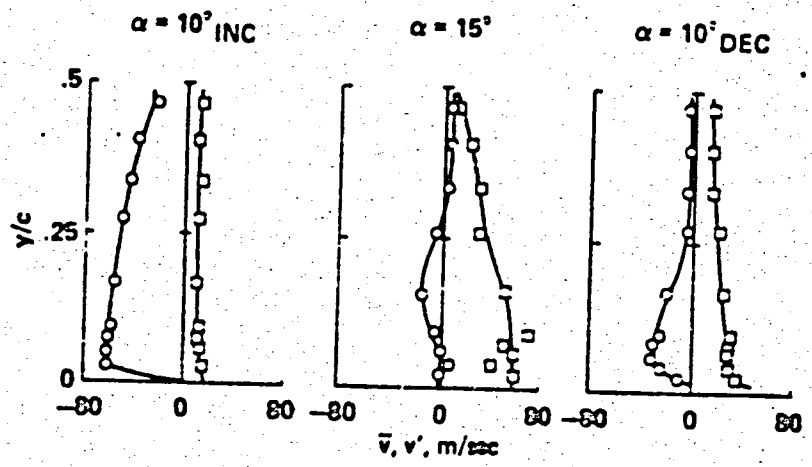

Fig 8 Ensemble-Averaged Vertical Mean and Turbulent Velocity Profiles at a Reduced Frequency of 0.12 (Circles Represent Mean Profiles)
x/c = 0.45

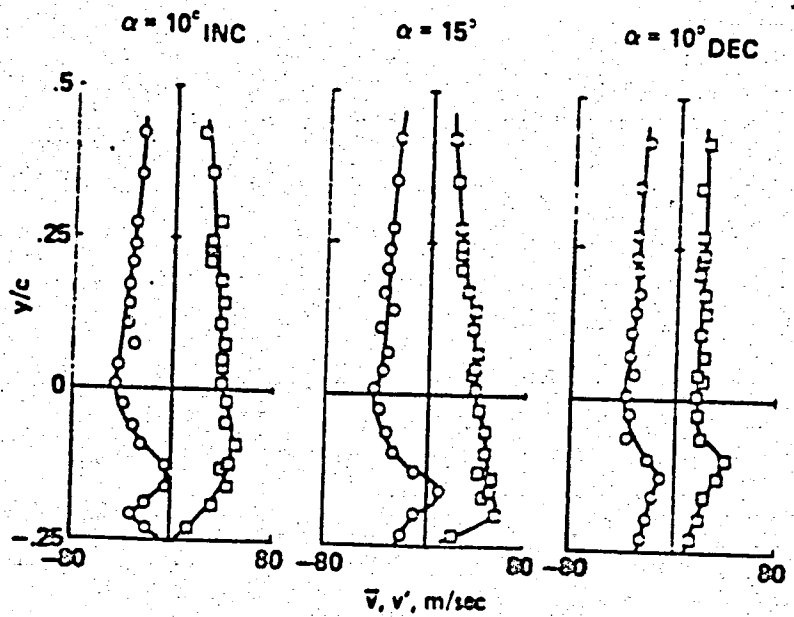

Fig. 9 Profiles for x/c = 1.06

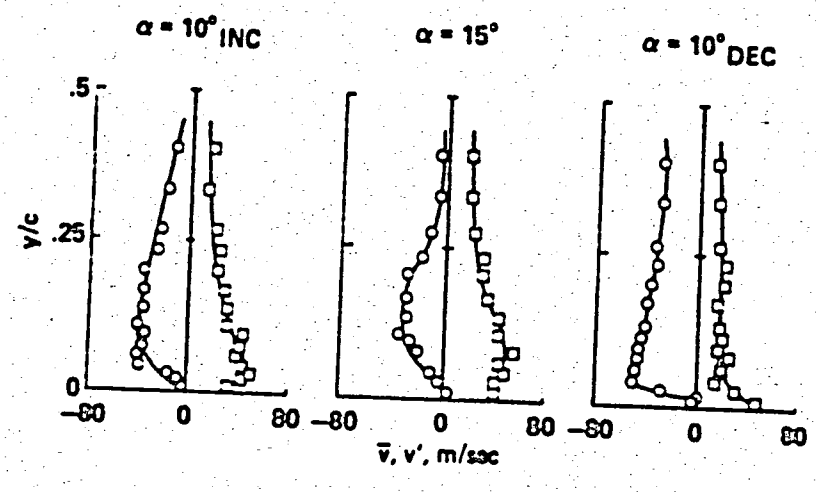

Fig. 10 Ensemble-Averaged Vertical Mean and Turbulent Velocity Profiles at a Reduced Frequency of 1.2 (Circles Represent Mean Profiles) x/c = 0.45

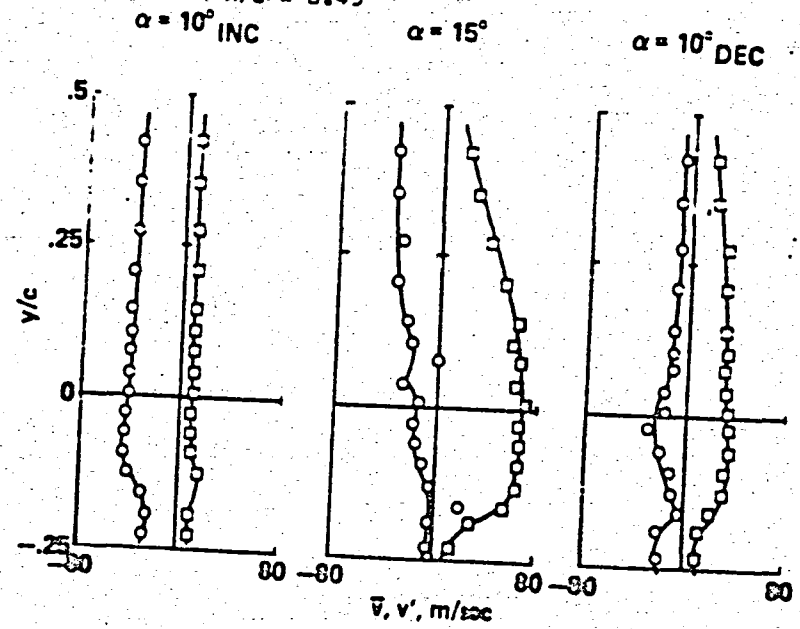

Fig. 11 Profiles for x/c = 1.06

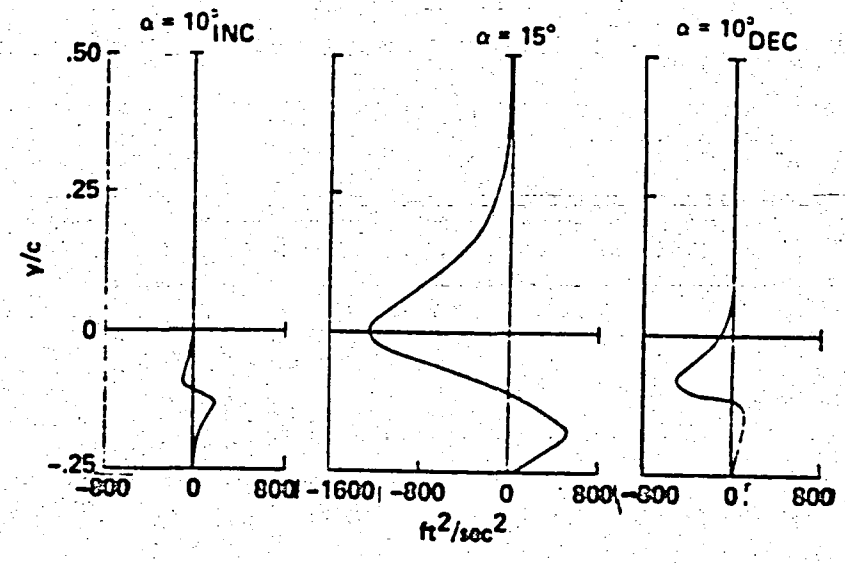

Fig. 12 Ensemble Averaged Reynolds Shear Stress Distributions for a Reduced Frequency of 0.12

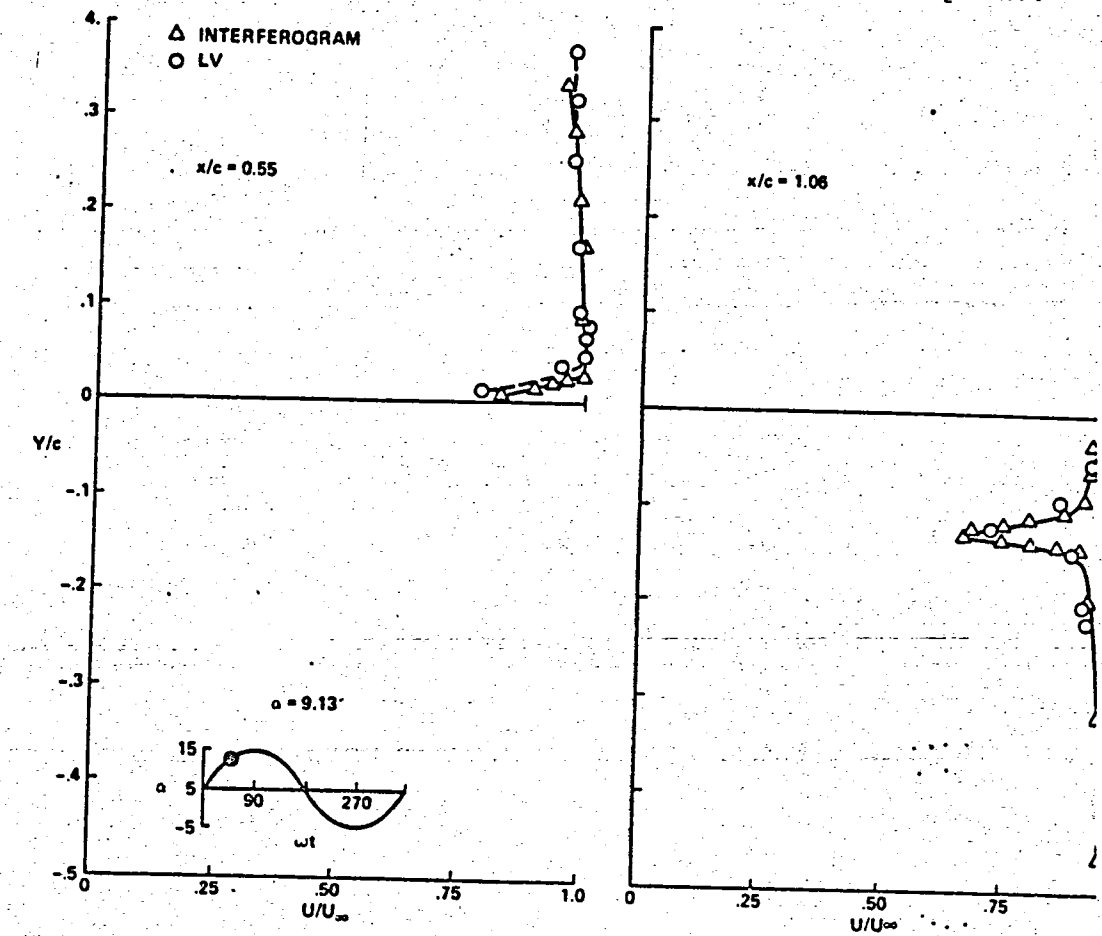

Fig. 13 Interferogram and Laser Velocimeter Comparison for Attached Flow (Ref. 1).

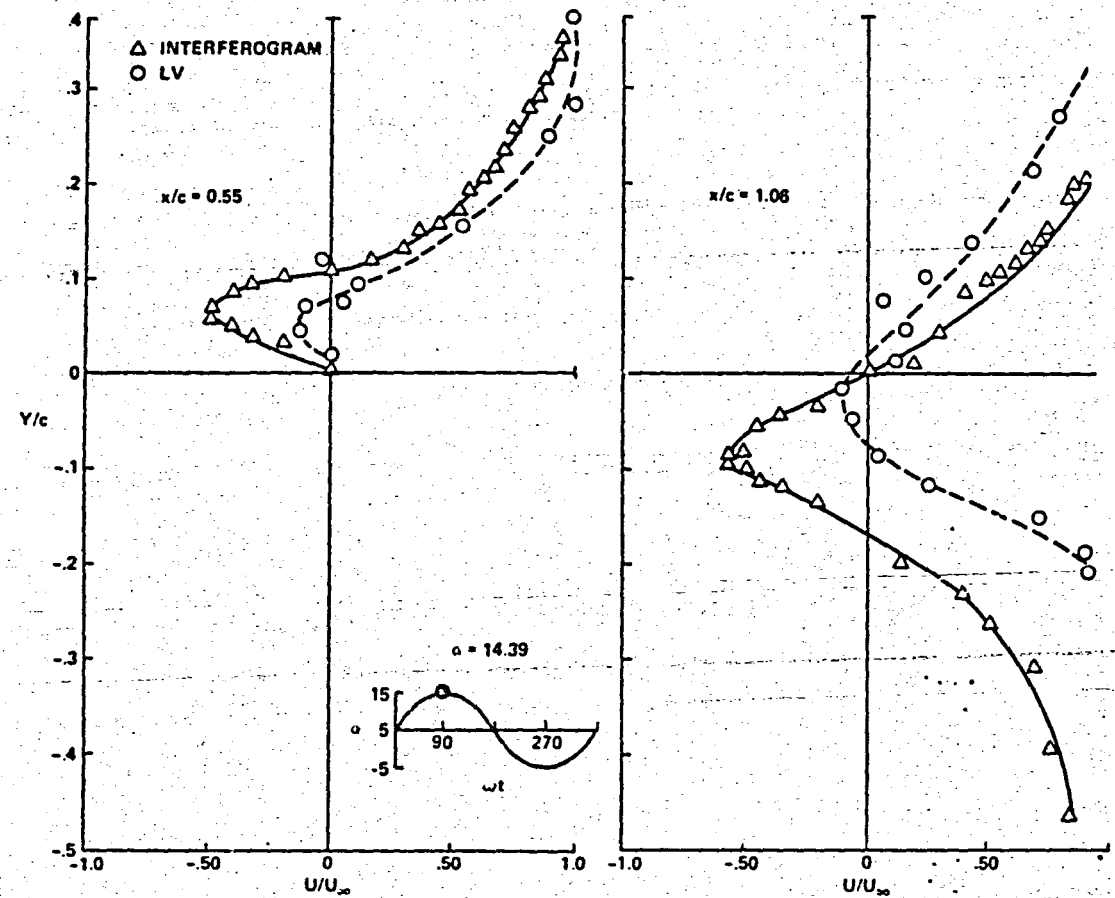

Fig. 14 Interferogram and Laser Velocimeter Comparison for Separated Flow (Ref. 1).

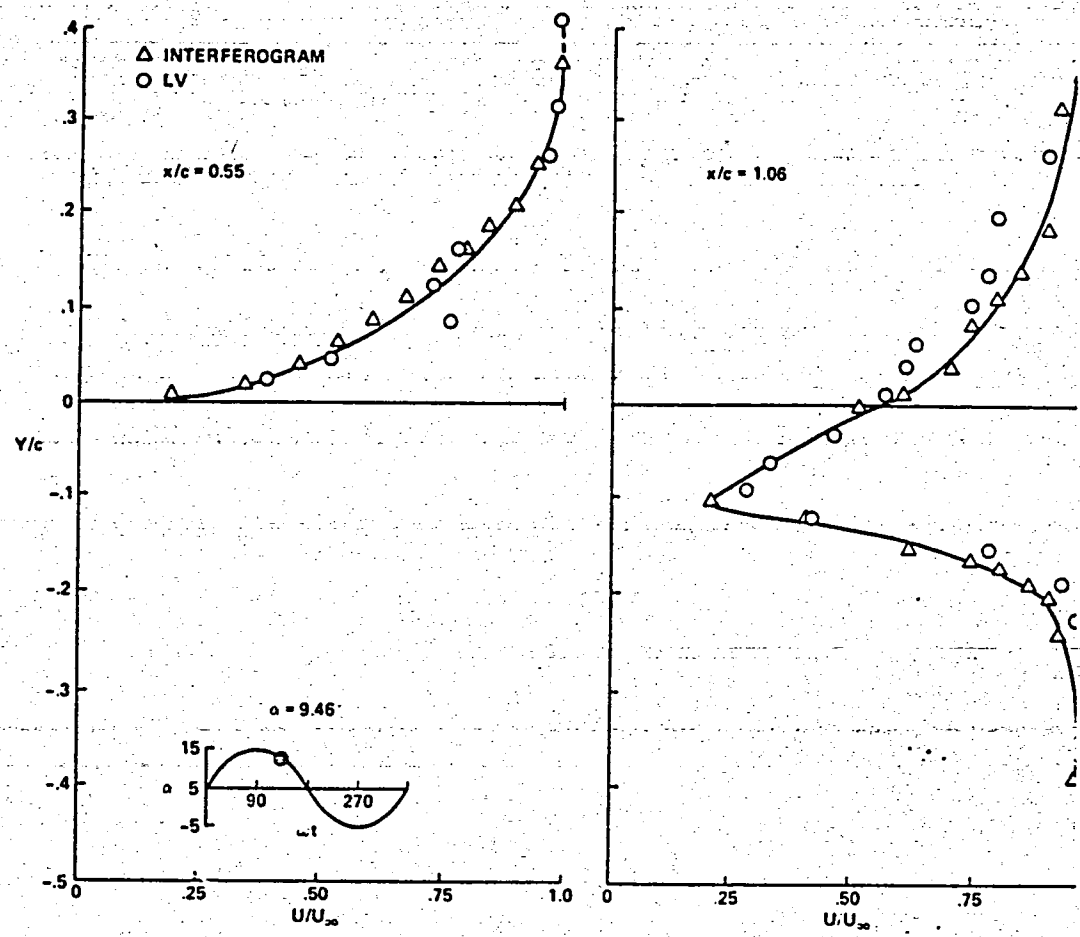

Fig. 15 Interferogram and Laser Velocimeter Comparison for Reattached Flow (Ref. 1).

END

DATE

FILMED

DEC 13 1984

End of Document